Enhancement Handling Performance of 4-Wheels Drive Electrical Vehicle Using Advanced Control Technique

Ahmed Hassan, Jose Ramon D. Frejo, Jose Maria Maestre
Dep. of Systems Engineering and Automation
Higher Technical School of Engineering, University of Seville
Av. de los Descubrimientos S/N, 41092 Seville
ahmhasahm@alum.us.es , jdominguez3@us.es , pepemaestre@us.es

Abstract

Electric vehicles (EVs) are gaining attention because they are environmentally friendly. Also, EVs can use in-hub motors, which can be independently controlled, improving maneuverability and allowing to set more ambitious control goals. In this paper, the lateral motion of an EV is controlled using the direct yaw control (DYC) method. The proposed controller uses the yaw moment produced by the longitudinal forces of the tires to stabilize the vehicle motion during critical cornering conditions to improve vehicle handling characteristics. The designed controllers, based on a linear model of the vehicle compute the optimal coupled traction/braking torque of the four in-wheel motors. By using unequal torque distribution, a restoring yaw moment can be generated in order to improve vehicle stability. Two controllers (PID and MPC) were designed to generate the moment required to achieve vehicle stability . The MPC outperforms PID regarding reduction of side slip angle and yaw rate.

Keywords: Model Predictive Control (MPC). Direct yaw moment (DYM). In-hub wheel motor (IWM).

1 Introduction

Due to the demand for vehicle security, numerous active safety systems have been developed to improve vehicle handling, stability and comfort[1], with many advanced control systems used in the production of modern vehicles.
This work focuses on vehicle handling and yaw stability control to overcome the problem that occurs when the lateral acceleration tire force approaches the adhesion limit and the vehicle side-slip angle increases. As a result, the steering is no longer capable of generating the desired yaw moment and the vehicle becomes laterally unstable as the yaw moment decreases at high values of side slip [2].
Significant research has been performed to generate a restoring moment by differential braking [3]. Individual controlled motors in electric vehicles powertrains are capable of enhancing the dynamic properties of the vehicle by distributing the wheel torques more freely [4]. Additionally, the use of in-wheel motors (IWM) provides new dynamics control opportunities [5]. In[6], for example, a DYC system was designed to control the angle of side slip to improve the handling and stability of a small-scale electric vehicle. In [7], the large vertical reaction force of IWM and the distribution of driving forces were used to independently control body roll and pitch motion . A novel direct yaw moment control system with cascaded traction and yaw stability control was proposed in [8], providing better adaptation to the road conditions and attenuating the yaw rate error. A forward type of tire force distribution control has been developed together with motion control of a complete drive-by-wire electric vehicle to improve vehicle stability and reduce tire energy dissipation caused by tire slip in [4]. Recently, the potential of the electric single-wheel drive has been studied to compensate for a rear-wheel-drive with a high rear axle load. A prototype vehicle with the main aim of showing the potential of single-wheel drive has been developed to demonstrate that it is indeed possible to reshape vehicle handling both in terms of steady-state understeering characteristics and transient response using torque vector control in [9][10].
This work is based on a prototype vehicle equipped with four electric motors hosted on the wheels, called Fox as in Figure 1.

Figure 1: The Fox vehicle.

This vehicle has been designed as a testing platform control with electric motor drives to directly control the torque given to the wheels and generate the yaw moment by providing unequal torques to the left and right wheels. The advantage of these motor drives is a quick response time and reduced system complexity.
Generally, the yaw rate and sideslip angle are chosen as control variables for such direct yaw control systems [11]. Various researchers have used different control methods such as Model Predictive

 https://doi.org/10.17979/spudc.9788497498418.0530

Control, Fuzzy Control, LQR Control, etc.
The main contribution of this paper is improving lateral stability control using optimal control techniques to enhance the handling performance of the vehicle and increase its safety by applying direct yaw method.
This paper is divided as follows. Sect.2 shows the linear and the non-linear model of the vehicle that were used to compute the optimal controller and to simulate the behavior of the vehicle, respectively. Sect.3 describes the optimal control techniques that have been used and torque vector control method as a low level control has been explained. Sect.4 summarizes and analyses the validation results. Finally, the conclusions are summarized in Sect.5.

2 Model of The Vehicle

Firstly, the linear model that has been used for the computation of the controller is a bicycle model. It is a two-degree-of-freedom model widely used due to its simplicity and good performance where the left and right wheels for each axis are merged and it has been used in [12]. The bicycle model is shown in Figure 2 with assumed moment M_z around the Z axis to maintain a balance with the applied forces.

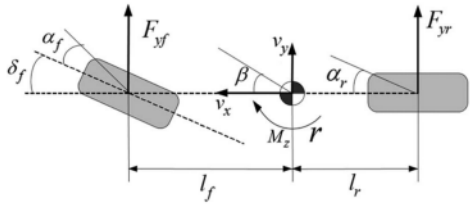

Figure 2: Vehicle Bicycle Model[13].

The equations of motion for the vehicle lateral dynamics are

$$mv_x(\dot{\beta} + r) = F_{yr} + F_{yf}, \tag{1}$$

$$I_z\dot{r} = l_f F_{yf} - l_r F_{yr} + M_z, \tag{2}$$

Where β is the vehicle side slip angle, m is the vehicle mass, r is the vehicle yaw rate, F_{yr} is the rear axle lateral tire force, F_{yf} is the front axle lateral tire force, v_x is vehicle longitudinal speed, l_r is the center of gravity (CG) to rear axle distance, l_f is (CG) to front axle distance, I_z is the vehicle yaw moment of inertia. In turning conditions, the dynamic equations of the bicycle will be linearized in such a way that we will only take into account small values of the lateral drift angles or the sideslip angles, where $\sin(\alpha) \approx \alpha$, $\cos(\alpha) \approx 1$. Where the lateral front and rear tire forces are simplified with the linear tire models as

$$F_{yf} = C_f\alpha_f, \tag{3}$$

$$F_{yr} = C_r\alpha_r, \tag{4}$$

where

$$\alpha_f = \delta_f - \left(\beta + \frac{l_f * r}{v_x}\right), \tag{5}$$

$$\alpha_r = -\beta + (\frac{l_f * r}{v_x}). \tag{6}$$

In (5) and (6), α_f and α_r are the slip angles of the front and rear tires, respectively; v_x is assumed to be constant for a short period of time. The dynamic tire model developed in [12] can be described as

$$\tau_{lag}\dot{F}_{(yf,lag)} + F_{(yf,lag)} = F_{yf}, \tag{7}$$

$$\tau_{lag}\dot{F}_{(yr,lag)} + F_{(yr,lag)} = F_{yr}, \tag{8}$$

where F_{yr_lag} and F_{yf_lag} are the lagged lateral tire forces of the front and rear tires, respectively, and τ_{lag} is the relaxation time constant defined as [14]

$$\tau_{lag} = \frac{\sigma}{v_x}. \tag{9}$$

Using the lagged tire forces (7) and (8), (1) and (2) can be rewritten as

$$mv_x(\dot{\beta} + r) = F_{(yf,lag)} + F_{(yr,lag)}, \tag{10}$$

$$I_z\dot{r} = l_f F_{(yf,lag)} - l_r F_{(yr,lag)} + M_z. \tag{11}$$

By augmenting (7) and (11), a vehicle model including the dynamic tire model can be obtained in state-space form as

$$\dot{x} = Ax + B_\delta\delta_f + B_M M_z, \tag{12}$$

where

$$x = \begin{bmatrix}\beta & \dot{\beta} & r & \dot{r}\end{bmatrix}^T,$$

$$\mathrm{A}= \begin{bmatrix} 0 & 1 & 0 & 0 \\ -\frac{C_f+C_r}{\tau_{lag}mv_x} & -\frac{1}{\tau_{lag}} & \left(\frac{C_r l_r - C_f l_f}{\tau_{lag}mv_x^2} - \frac{1}{\tau_{lag}}\right) & -1 \\ 0 & 0 & 0 & 1 \\ \frac{C_r l_r - C_f l_f}{\tau_{lag}I_z} & 0 & -\frac{C_f l_f^2 + C_r l_r^2}{\tau_{lag}I_z v_x} & -\frac{1}{\tau_{lag}} \end{bmatrix},$$

$$\mathrm{B}_\delta = \begin{bmatrix} 0 \\ \frac{C_f}{\tau_{lag}mv_x} \\ 0 \\ \frac{C_f l_f}{\tau_{lag}I_z} \end{bmatrix}, B_M = \begin{bmatrix} 0 \\ 0 \\ 0 \\ \frac{1}{\tau_{lag}I_z} \end{bmatrix}. \tag{13}$$

In [15] the validation of the linear model has been performed using a nonlinear model implemented in Simmechanics. In Matlab, the test consists of keeping the steering wheel straight and applying a certain angular momentum to the vehicle on the Z-axis by generating torques on the axes. This emulates the operation of the controller since this tells us what angular momentum we should apply to the vehicle as follows:

https://doi.org/10.17979/spudc.9788497498418.0530

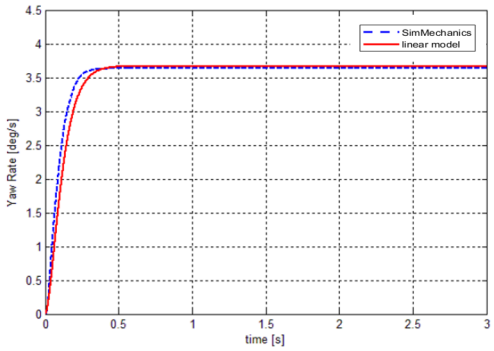

Figure 3: Angular velocity comparison.

This test has been done at $Mz = 550$ $[kg.m^2.rad/s]$ and at a speed of 70 $[km/h]$ as shown in Figure 3.

The non-linear model was presented and validated in [14].

3 Control Formulation

Two controllers (PID, MPC) are developed as high-level control to generate the corrective yaw moment required to achieve vehicle stability and then use torque vector control as low-level control to distribute the required torque for each motor as shown in Figure 5 .

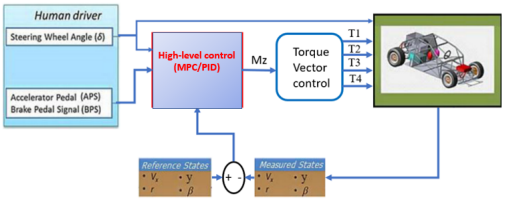

Figure 4: The general Simulink block of the used controllers

3.1 Torque Vector controller (TVC)

It is the low-level control used for torque calculation and this control is responsible for distributing the torque required for each motor [16].

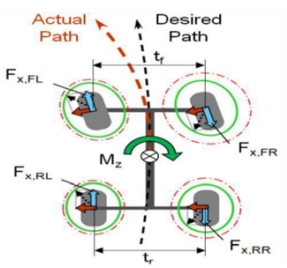

Figure 5: TVC's distribution [17].

As shown in Figure 5, the TVC is responsible for distributing the torque between the four motors to generate the desired angular momentum, thus acting as a low-level controller by dividing the generated the angular momentum as

$$M_z = M_{z,front} + M_{z,rear} = 0.5M_z + 0.5M_z, \quad (14)$$

$$M_{z,front} = F_{x,fr}\frac{t_f}{2} + F_{x,fl}\frac{t_f}{2}, \quad (15)$$

The longitudinal forces on right and left sides are distributed as in [18] according to the vertical forces and road friction based on the friction circle μ as :

$$F_{x,f} = \sqrt{(\mu F_z)^2 - F_y^2}, \quad (16)$$

$$F_{x,f} = \frac{M_{z,front}}{t_f}. \quad (17)$$

By doing the same for the rear ones, we have

$$F_{x,r} = \frac{M_{z,rear}}{t_r}, \quad (18)$$

The high-level controller obtains the required angular momentum that must be applied to the vehicle to correct its trajectory, where $F_{x,fr}, F_{x,fl}, F_{x,rr}, F_{x,rl}$ are the longitudinal forces of the front-right, front-left, rear-right, and rear-left wheels, respectively,and t_f, t_r are the width of the front and rear axles. The required torque from the electric motor is obtained as

$$T_m - F_x r_{dyn} = I_{yy}\dot{\omega}, \quad (19)$$

$$T_{m,i} = \frac{r_{dyn}}{t_f}M_{z,front} + I_{yy}\dot{\omega}, \quad (20)$$

where T_m is the torque generated by the electric motor, r_{dyn} is the dynamic radius of the tire although in our case for simplicity it is assumed constant, I_{yy} is the moment of inertia of the wheel on its axis turning and ω is the angular speed of the wheel. To derive a linear steady state (ss) reference model, all time-varying parameters $(\dot{\beta}, \dot{r})$ were considered equal to zero [19]. The side of the reference vehicle can be considered zero for higher stability and better tracking performance [20]:

$$\beta_{des} = 0, \quad (21)$$

with the assumption that the car is describing a curvilinear trajectory constant turning radius (R) with a dynamic stationary that keeps the value of speed(V), angular velocity (r) and angle sideslip β without changes means $[\dot{r} = 0]$ and $[\dot{\beta} = 0]$. With these considerations, the angular velocity is

$$r_{des} = \frac{V}{L + \frac{m}{L}(\frac{b}{C_{\alpha f}} - \frac{a}{C_{\alpha r}})V^2}\delta \quad (22)$$

Equation (22) shows the relationship between the angular velocity of the vehicle and the angle of rotation of the front wheels in a stationary state.

https://doi.org/10.17979/spudc.9788497498418.0530

3.2 The MPC controller

MPC is a type of optimal control that uses a model of a process to predict the system evaluation and find a set of optimal inputs that minimize the given function while satisfying constraints over a specified time horizon. Only the first input in the sequence of optimal inputs is applied to the system at each time step [21]. MPC is a receding horizon strategy and has become very successful in the industry, mainly due to its ability to handle constraints. To form an MPC problem, the bicycle model was discretized using zero-order hold as follows.

$$\begin{aligned} x_k(t) &= A_{mpc}x_k(t-1) + B_{mpc}u_k(t-1), \\ y_k(t) &= C_{mpc}x_k(t). \end{aligned} \tag{23}$$

where

$$u_k(t-1) = M_{z,k}(t-1) \tag{24}$$

Subscript k denotes that the corresponding discretized matrices are at the kth step in discrete time. An incremental formulation is used, where the control signal now happens to be $\Delta U_k(t) = U_k(t) - U_k(t-1)$. The system equations are as follows:

$$\begin{bmatrix} x_k(t+1) \\ u_k(t) \end{bmatrix} = \begin{bmatrix} A_{mpc} & B_{mpc} \\ 0 & I \end{bmatrix} \cdot \begin{bmatrix} x_k(t) \\ u_k(t-1) \end{bmatrix} + \begin{bmatrix} B_{mpc} \\ I \end{bmatrix} .\Delta u \tag{25}$$

$$y(t) = \begin{bmatrix} C_{mpc} & 0 \end{bmatrix} \cdot \begin{bmatrix} x_k(t) \\ u_k(t-1) \end{bmatrix} \tag{26}$$

To simplify the previous expressions, it is defined A new extended state vector as:
$\bar{x} = \begin{bmatrix} x(t) & u(t-1) \end{bmatrix}^T$
Which leads to

$$\begin{aligned} \bar{x}(t+1) &= M\bar{x}(t) + N\Delta u(t) \\ y(t) &= Q\bar{x}(t) \end{aligned} \tag{27}$$

Here, the relationship between the matrices M, N and Q and the non-incremental matrices A, B and C remains as extended state vector and vector deviations:

$$\begin{aligned} \bar{x}(t) &= \begin{bmatrix} \beta(t) & \dot{\beta}(t) & r(t) & \dot{r}(t) & \delta(t) & M_z(t-1) \end{bmatrix}^T \\ y(t) &= \begin{bmatrix} \beta(t) & r(t) \end{bmatrix}^T \end{aligned} \tag{28}$$

In these expressions,M_z is included in U, there is the sideslip angle (β), the angular velocity around the Z axis r, the angle of rotation of the front wheels (δ) and the angular moment that it is necessary to apply to the vehicle to correct the dynamic (M_z). Using the incremental model, the following outputs are obtained as

$$\hat{y}(t+j) = QM^j\hat{x}(t) + ... + \sum_{i=0}^{j-1} QM^{j-i-1}N\Delta u(t+i). \tag{29}$$

It should be noted that all states are measurable $\hat{x}(t)$. By following [22], the cost function of MPC is defined as follows:

$$J = (Hu + F\hat{x}(t) - w)^T(Hu + F\hat{x}(t) - w) + ... + \lambda u^T u \tag{30}$$

the optimal control action can be obtained as

$$u = (H^T H + \lambda I)^{-1} H^T (w - F.\dot{x}(t))u \tag{31}$$

Following [15] [22] for more details.

4 Simulation Results

In this section, we present the results of the simulation. ISO 3888 or the double change lane maneuver has been chosen as the standard test, which is a closed-loop test that evaluates the stability of the vehicle as shown in Figure 6.

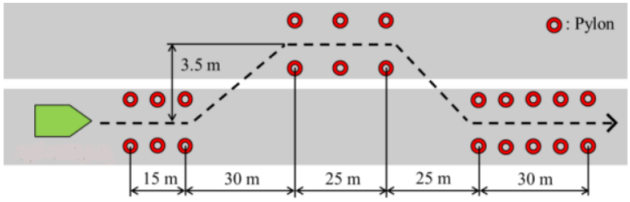

Figure 6: The double change lane(ISO 3888)

It is a common test that is used to indicate the capabilities of a vehicle to manage a curve and evaluate the designed control system. The simulation was carried out in the Simmechanics environment. The required outputs (such as the yaw rate and side slip angle) and also other parameters have been computed to evaluate the control system as shown in Figures 7- 12:

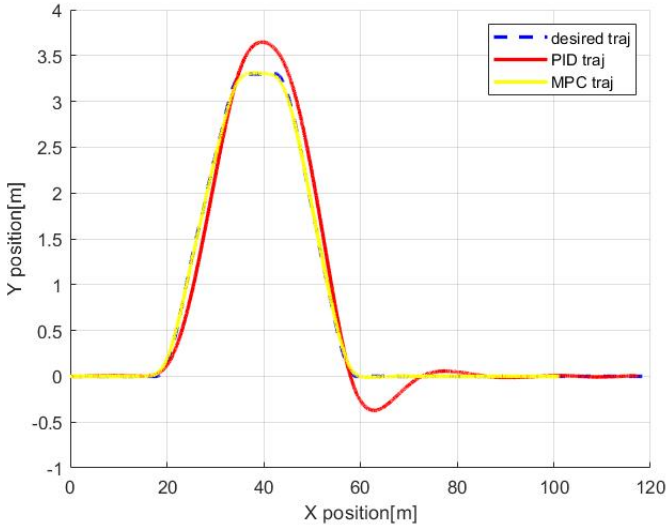

Figure 7: The vehicle's trajectory

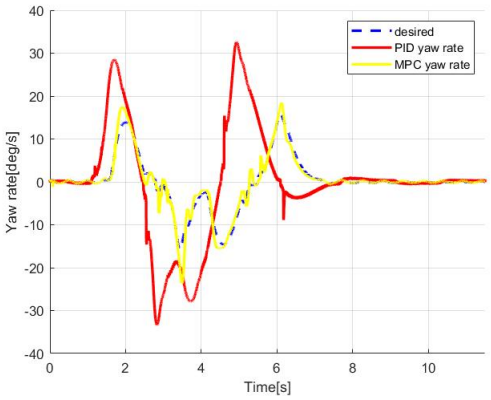

Figure 8: The yaw rate response

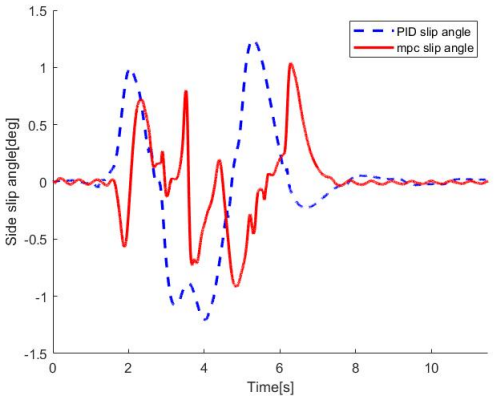

Figure 9: The side slip response

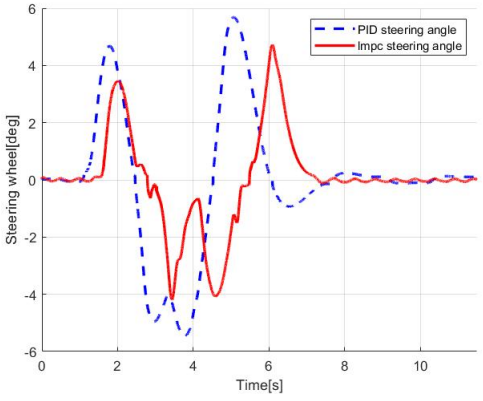

Figure 10: steering wheel

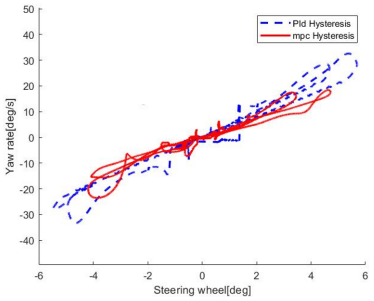

Figure 11: Hysteresis response

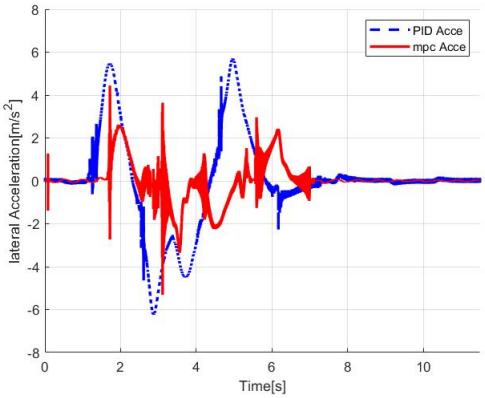

Figure 12: Lateral Acceleration

Figure 7 shows the trajectory followed by the vehicle with the PID and the MPC controllers. The MPC controller was able to follow the required trajectory with a low tracking error. Figures 8 and 9 represent the evaluation of the angular speed and the angle side slip. The MPC controller gave results closer to the required values. The designed MPC controller was also, able to prevent the occurrence of an oscillation yielding smoother behavior for the driver. This is relevant to avoid accidents, as sudden maneuvers on the road usually result in this phenomenon. Regarding side slip, with the PID controller, the maximum values are approximately in the range [-1.4 , 1.4] degrees. With the MPC controller, range is reduced to approximately [-1 , 1] degree, which guarantees better maneuverability and predictability. Finally, in Figure 10, a comparison has been made between the steering wheel obtained with each controller. With the PID controller, the range becomes [-6 , 6] degrees. On the other hand, the MPC controller, the extreme values are reduced to [-4 , 4] degrees. In Figure 11, the evaluation of hysteresis was obtained by measuring the relation between the yaw rate and the angle of the steering wheel. In general, the definition of hysteresis is the energy lost and not returned when tires are subjected to stress in any direction. Lost energy is converted to

https://doi.org/10.17979/spudc.9788497498418.0530

heat through molecular interaction and since rubber has poor thermal conductivity, the internal temperatures of a tire can accumulate rapidly under repeated flexing. Usually, for simulation studies, hysteresis is expressed as a time delay or as linear functions. The width of this curve shows the relation between the value of the steering wheel and the capacity of vehicle response, how closer the vehicle becomes to it; there is a lower delay between the steering wheel and the time it takes the vehicle to spin. This is very important, since delayed systems are difficult to control. As noted in Figure 11, the width and length of the MPC curve is less than that of PID, so the car behavior can be easily managed and easily controlled. In Figure 12, the last variable is lateral acceleration. The MPC was able to reduce the peak value of lateral acceleration with respect to the PID controller. This increases the security and comfort of the driver.

5 Conclusions and Future work

In this paper, two controllers (PID and MPC) have been designed to achieve yaw stability for the four-wheel drive vehicle. The linearized model of the vehicle obtained was used by the predictive controller to capture the future behavior of the car. The MPC controller has better results related to the yaw rate and side slip angle and it also has many advantages comparing to the PID such as the inclusion constraints. In future works, the controllers obtained will be tested and applied to the real vehicle shown in Figure 13, also the a non-linear MPC will be proposed and tested.

Figure 13: experimental test

Acknowledgement

Financial support for this research was provided by the Spanish Ministry of Scince and Innovation (Grant no.IJC2018-035395-I).

References

[1] Moustapha Doumiati, Olivier Sename, Luc Dugard, John-Jairo Martinez-Molina, Peter Gaspar, and Zoltan Szabo. Integrated vehicle dynamics control via coordination of active front steering and rear braking. *European Journal of Control*, 19(2):121–143, 2013.

[2] Husain Kanchwala, Johan Wideberg, Carlos Bordons Alba, and David Marcos. Control of an independent 4wd electric vehicle by dyc method. *International Journal of Vehicle Systems Modelling and Testing*, 10(2):168–184, 2015.

[3] Lin Zhang, Haitao Ding, Yanjun Huang, Hong Chen, Konghui Guo, and Qin Li. An analytical approach to improve vehicle maneuverability via torque vectoring control: theoretical study and experimental validation. *IEEE Transactions on Vehicular Technology*, 68(5):4514–4526, 2019.

[4] Yuta Suzuki, Yoshio Kano, and Masato Abe. A study on tyre force distribution controls for full drive-by-wire electric vehicle. *Vehicle System Dynamics*, 52(sup1):235–250, 2014.

[5] Satoshi Murata. Innovation by in-wheel-motor drive unit. *Vehicle System Dynamics*, 50(6):807–830, 2012.

[6] P Raksincharoensak, M Kamata, M NAGAI, et al. Side slip control of small-scale electric vehicle by dyc. In *THE DYNAMICS OF VEHICLES ON ROADS AND ON TRACKS. PROCEEDINGS OF THE 18TH IAVSD SYMPOSIUM HELD IN KANAGAWA, JAPAN, AUGUST 24-30, 2003*, 2004.

[7] Etsuo Katsuyama. Decoupled 3d moment control using in-wheel motors. *Vehicle System Dynamics*, 51(1):18–31, 2013.

[8] Hiroshi Fujimoto, Akio Tsumasaka, and Toshikuni Noguchi. Vehicle stability control of small electric vehicle on snowy road. *Review of automotive engineering*, 27(2):279–286, 2006.

[9] Alfred Pruckner, Elsa Davy, Dirk Schlichte, and Stephan Kaspar. Electric single wheel drive optimised installation space at maximum vehicle dynamics. *ATZ worldwide*, 116(3):28–33, 2014.

[10] Alfred Pruckner, Stephan Kaspar, Ralf Stroph, and Christoph Grote. Vehicle dynamics per software–potentials of an electric single wheel drive. In *Conference on Future Automotive Technology*, pages 147–165. Springer, 2013.

[11] Matthew Brown, Joseph Funke, Stephen Erlien, and J Christian Gerdes. Safe driving envelopes for path tracking in autonomous ve-

hicles. *Control Engineering Practice*, 61:307–316, 2017.

[12] Hans Pacejka. *Tire and vehicle dynamics*. Elsevier, 2005.

[13] Mooryong Choi and Seibum B Choi. Model predictive control for vehicle yaw stability with practical concerns. *IEEE Transactions on Vehicular Technology*, 63(8):3539–3548, 2014.

[14] David Marcos Rodríguez. *Contributions to power management and dynamics control in hybrid vehicles*. PhD thesis, Universidad de Sevilla, 2014.

[15] G Hernández Rodríguez and C Bordons Alba. Control de estabilidad basado en mpc para un vehículo eléctrico con motores en rueda. *Sevilla: Universidad de Sevilla*, 2015.

[16] Kiumars Jalali. Stability control of electric vehicles with in-wheel motors. 2010.

[17] Gonzalo Hernández, Carlos Bordons Alba, David Marcos, and Carlos Montero. Control de estabilidad basado en mpc para un vehículo eléctrico con motores en rueda. *Jornadas de automática (2015), p 887-894*, 2015.

[18] Ossama Mokhiamar and Masato Abe. Simultaneous optimal distribution of lateral and longitudinal tire forces for the model following control. *J. Dyn. Sys., Meas., Control*, 126(4):753–763, 2004.

[19] Rajesh Rajamani. *Vehicle dynamics and control*. Springer Science & Business Media, 2011.

[20] Hong Wang, Yanjun Huang, Amir Khajepour, Yubiao Zhang, Yadollah Rasekhipour, and Dongpu Cao. Crash mitigation in motion planning for autonomous vehicles. *IEEE transactions on intelligent transportation systems*, 20(9):3313–3323, 2019.

[21] Mansour Ataei. Reconfigurable integrated control for urban vehicles with different types of control actuation. 2017.

[22] Eduardo F Camacho and Carlos Bordons. Introduction to model predictive control. In *Model Predictive Control*, pages 1–11. Springer, 2007.

 https://doi.org/10.17979/spudc.9788497498418.0530